THE JOURNAL OF BIOLOGICAL CHEMISTRY VOL. 285, NO. 48, pp. 37458–37466, November 26, 2010

Golgi Calcium Pump Secretory Pathway Calcium ATPase 1 (SPCA1) Is a Key Regulator of Insulin-like Growth Factor Receptor (IGF1R) Processing in the Basal-like Breast Cancer Cell Line MDA-MB-231*

Received for publication, July 11, 2010, and in revised form, August 3, 2010 Published, JBC Papers in Press, September 13, 2010, DOI 10.1074/jbc.M110.163329

Desma M. Grice[‡], Irina Vetter[§], Helen M. Faddy[‡], Paraic A. Kenny[¶1], Sarah J. Roberts-Thomson[‡2], and Gregory R. Monteith[‡2,3]

From the [‡]School of Pharmacy and [§]Institute for Molecular Bioscience, University of Queensland, Brisbane 4072, Australia and the [¶]Department of Developmental and Molecular Biology, Albert Einstein College of Medicine, Bronx, New York 10461

Calcium signaling is a key regulator of pathways important in tumor progression, such as proliferation and apoptosis. Most studies assessing altered calcium homeostasis in cancer cells have focused on alterations mediated through changes in cytoplasmic free calcium levels. Here, we show that basal-like breast cancers are characterized by an alteration in the secretory pathway calcium ATPase 1 (SPCA1), a calcium pump localized to the Golgi. Inhibition of SPCA1 in MDA-MB-231 cells produced pronounced changes in cell proliferation and morphology in three-dimensional culture, without alterations in sensitivity to endoplasmic reticulum stress induction or changes in global calcium signaling. Instead, the effects of SPCA1 inhibition in MDA-MB-231 cells reside in altered regulation of calcium-dependent enzymes located in the secretory pathway, such as proprotein convertases. Inhibition of SPCA1 produced a pronounced alteration in the processing of insulin-like growth factor receptor (IGF1R), with significantly reduced levels of functional IGF1Rβ and accumulation of the inactive trans-Golgi network pro-IGF1R form. These studies identify for the first time a calcium transporter associated with the basal-like breast cancer subtype. The pronounced effects of SPCA1 inhibition on the processing of IGF1R in MDA-MB-231 cells independent of alterations in global calcium signaling also demonstrate that some calcium transporters can regulate the processing of proteins important in tumor progression without major alterations in cytosolic calcium signaling. Inhibitors of SPCA1 may offer an alternative strategy to direct inhibitors of IGF1R and attenuate the processing of other proprotein convertase substrates important in basal breast cancers.

Calcium levels within a cell control a variety of cellular processes relevant to tumorigenesis such as proliferation, migration, and apoptosis (1, 2). Although cellular calcium homeostasis is precisely controlled, there is an emerging appreciation that it is remodeled during cancer with downstream consequences on cellular function (3). Deregulation of calcium homeostasis may arise via changes in calcium-transporting proteins such as channels and pumps whose expression can be up- or down-regulated in cancers (2). Expression changes in these calcium transporters may modulate global cytosolic calcium levels and/or due to their location may alter only the calcium levels, in particular intracellular calcium stores, *e.g.* the Golgi (2, 4, 5). Within the Golgi reside calcium-regulated enzymes, such as the proprotein convertases that have been described as master switches in tumorigenesis (6), and whose substrates include insulin-like growth factor receptor (IGF1R),[4] a protein linked epidemiologically, clinically, and experimentally to breast cancer (7). The identification of regulators of proprotein convertases, such as regulators of Golgi luminal calcium levels, would be important therapeutically as they may offer an alternative means to globally control these pathways.

One regulator of Golgi luminal calcium levels is the secretory pathway calcium ATPase 1 (SPCA1), an active transporter of calcium into the secretory pathway (8–11). Mutations in *SPCA1* (*ATP2C1*) manifest as Hailey Hailey disease, an autosomal dominant skin disorder (12). Hailey Hailey disease is characterized only by symptoms involving stratified squamous epithelium that arise due to loss of cell to cell adhesion (acantholysis) (13). Different mutations in *ATP2C1* have been documented across families with Hailey Hailey disease, the commonality being a decrease in SPCA1 expression (8, 14, 15). Within the cell, SPCA1 inhibition appears to alter the cell surface levels of exogenously expressed proteins suggesting a functional consequence of SPCA1 in protein trafficking (10). Physiologically, SPCAs appear to have important roles in the mammary gland and likely contribute to the secretion of calcium into milk (16–18). Although the Golgi apparatus does not appear to be a major site of calcium storage, in most cells it is suggested to have a more prominent role in specialized secre-

* This work was supported in part by Cancer Council of Queensland Grant 569644, National Health and Medical Research Council of Australia Grant 631347, and an Australian postgraduate award (to D. M. G. and H. M. F.).
[1] Supported by Susan G. Komen for the Cure Grant KG100888 and Department of Defense CDMRP Breast Cancer Research Program Grant W81XWH-09-1-0680.
[2] Both authors should be considered as senior authors.
[3] To whom correspondence should be addressed. Tel.: 61-7-3346-1855; E-mail: gregm@uq.edu.au.

[4] The abbreviations used are: IGF1R, insulin-like growth factor receptor; $[Ca^{2+}]_{CYT}$, cytosolic calcium; CPA, cyclopiazonic acid; ER, endoplasmic reticulum; PAR, protease-activated receptor; PMCA, plasma membrane calcium ATPase; pro-IGF1R, pro- insulin-like growth factor receptor; siNT, nontargeting siRNA; siSPCA1, SPCA1 siRNA; SPCA1, secretory pathway calcium ATPase; TGN, trans-Golgi network; ANOVA, analysis of variance; BAPTA, 1,2-bis(2-aminophenoxy)ethane-*N*,*N*,*N*′,*N*′-tetraacetic acid.

tory cells, such as those of the mammary gland (19). Despite this important physiological role, there is a paucity of data regarding the pathophysiological consequences of SPCA1 in the breast.

Disruption of normal SPCA1 activity could modify calcium levels in the cytosol and/or within the Golgi lumen, both with consequences on calcium signaling although different pathways. There have been very few studies addressing the consequences of SPCA1 inhibition on cytosolic calcium changes produced by cell stimuli. SPCA1 silencing in HeLa cells has only relatively minor effects on cytosolic calcium responses produced by histamine (20); however, in spermatozoa, SPCA1 appears to play a major role in the regulation of cytosolic calcium transients (21).

Cytosolic calcium levels have demonstrated effects on cellular functions, including proliferation, gene expression, and contractility (1). However, the consequences of altered Golgi luminal calcium levels in mammalian cells are relatively unexplored. The Golgi is responsible for the post-translational modification of proteins prior to secretion, for example glycosylation of proteins (22). Disruption of *CaPMR1*, the *Candida albicans* homolog of SPCA, causes a gross defect in glycosylation (23), and siRNA inhibition of SPCA1 in mammalian cells results in a defect in the post-translational modification of the secretory glycoprotein thyroglobulin (24). Calcium levels within the Golgi lumen are likely to regulate other calcium-dependent enzymes, including the proprotein convertases. Indeed, in the yeast *Yarrowia lipolytica,* there is one report of *YlPMR1* (secretory pathway calcium ATPase homolog) regulating the processing of the proprotein convertase substrate alkaline extracellular protease (25). Proprotein convertase substrates have a significant role in cancer (6), and as yet there are no studies investigating the link between SPCA1, calcium-regulated proprotein convertases, and cancer.

Insulin-like growth factor receptor (IGF1R) is a proprotein convertase substrate important for mammary gland development and milk production (26, 27). Expression of IGF1R is increased in breast cancers and is associated with cancer initiation, evasion of apoptosis, motility, proliferation, and resistance to cancer therapy (7, 28). Suggesting a possible association with breast cancers of the poorest prognosis, IGF1R expression is significantly higher in those tumors from women with BRCA1 mutations compared with those tumors from women without BRCA1 mutations (29). Mice overexpressing *IGF1R* and constitutively active Kras develop mammary gland tumors of the basal-like subtype (30). Basal-like breast tumors are classified as such on the basis of their gene expression profile (31). Often, basal-like breast tumors have alterations in BRCA1, and they are associated with a poor outcome and a paucity of therapeutic options (32).

Here, we studied the possible association of SPCA1 with different breast cancer subtypes and the functional consequences of loss of SPCA1 in a breast cancer cell line. Our results identify SPCA1 as the first calcium transporter associated with basal-like breast cancers. We also saw pronounced effects of SPCA1 inhibition on MDA-MB-231 basal breast cancer cells that were independent of global effects on cytosolic calcium and identified SPCA1 as a key regulator of IGF1R processing in basal breast cancer cells. SPCA1 modulation and regulation of Golgi calcium transport may provide a unique opportunity for therapeutic targeting of this important pathway in breast cancer. This work redefines the potential role of calcium transporters in tumorigenesis by identifying critical roles in cancer-relevant pathways that occur independently of changes in global calcium signaling.

EXPERIMENTAL PROCEDURES

Cell Culture—MDA-MB-231 cells were routinely cultured in high glucose Dulbecco's modified Eagle's medium (Invitrogen) containing streptomycin sulfate/penicillin (100 μg/ml and 100 units/ml; Invitrogen), fetal bovine serum (10%; JRH Biosciences), and L-glutamine (4 mM; ThermoTrace) and maintained at 37 °C in a humidified 5% CO_2, 95% air incubator. Cell lines were routinely tested for mycoplasma contamination and monitored for morphological characteristics.

Microarray Analysis—SPCA1 expression was assessed in breast cancer clinical samples and cell lines in a dataset obtained from Rosetta Inpharmatics consisting of the microarray profiles of 295 primary breast tumors (33) and an Affymetrix microarray dataset of breast cancer cell lines classified as basal-like or luminal as described previously (34, 35). For Affymetrix data, the probe 209935_at was assessed. Array data were analyzed using Partek Genomics Suite (Partek Inc.), and subsequent statistical analysis was conducted using Prism 5 (GraphPad Inc.). In both cases, the median level of SPCA1 was compared between the sample groups. Statistical significance was determined using the Mann-Whitney test (for two sample groups) and the Kruskall-Wallis test with Dunn's post-test (for more than two sample groups). p values of < 0.05 were considered significant. SPCA1 expression was further analyzed using microarray breast cancer studies available at Oncomine™ (Compendia Bioscience, Ann Arbor, MI).

Silencing of Gene Expression—ON-TARGET *plus* Smartpool siRNAs (consists of four pooled siRNAs) were purchased from Dharmacon (Millennium Science, Australia). MDA-MB-231 cells were plated at 2500 cells/well into 96-well plates and treated with SPCA1 siRNA (100 nM; siSPCA1; L-006119-00), nontargeting siRNA (siNT) or transfection agent only (mock) using DharmaFECT 4 according to the manufacturer's instructions. RNA was isolated at the time points depicted in the figures, and protein was isolated at 72 h post-siRNA treatment.

Real Time RT-PCR—Total RNA was isolated using the RNeasy Plus mini kit (Qiagen), and mRNA was quantitated using real time RT-PCR and a 7500 real time PCR system (Applied Biosystems). SPCA1 and GRP94 were amplified using the TaqMan® gene expression assays Hs00205122_m1 and Hs00427665_g1, respectively, and data were normalized to 18 S rRNA and analyzed using the comparative C_t method as described previously (36).

Immunoblotting—Protein was isolated as described previously (36) and separated via SDS-PAGE prior to transfer to a PVDF membrane and probing with either mouse monoclonal anti-SPCA1 (1:500; H00027032-M01; Abnova), monoclonal anti-PMCA (1:2000; 5F10; Affinity Bioreagents), or monoclonal anti-SERCA2 (1:1000; MA3-910; Affinity Bioreagents) and anti-mouse β-actin (1:10,000; A5441; Sigma) followed by a goat anti-mouse HRP-conjugated secondary antibody

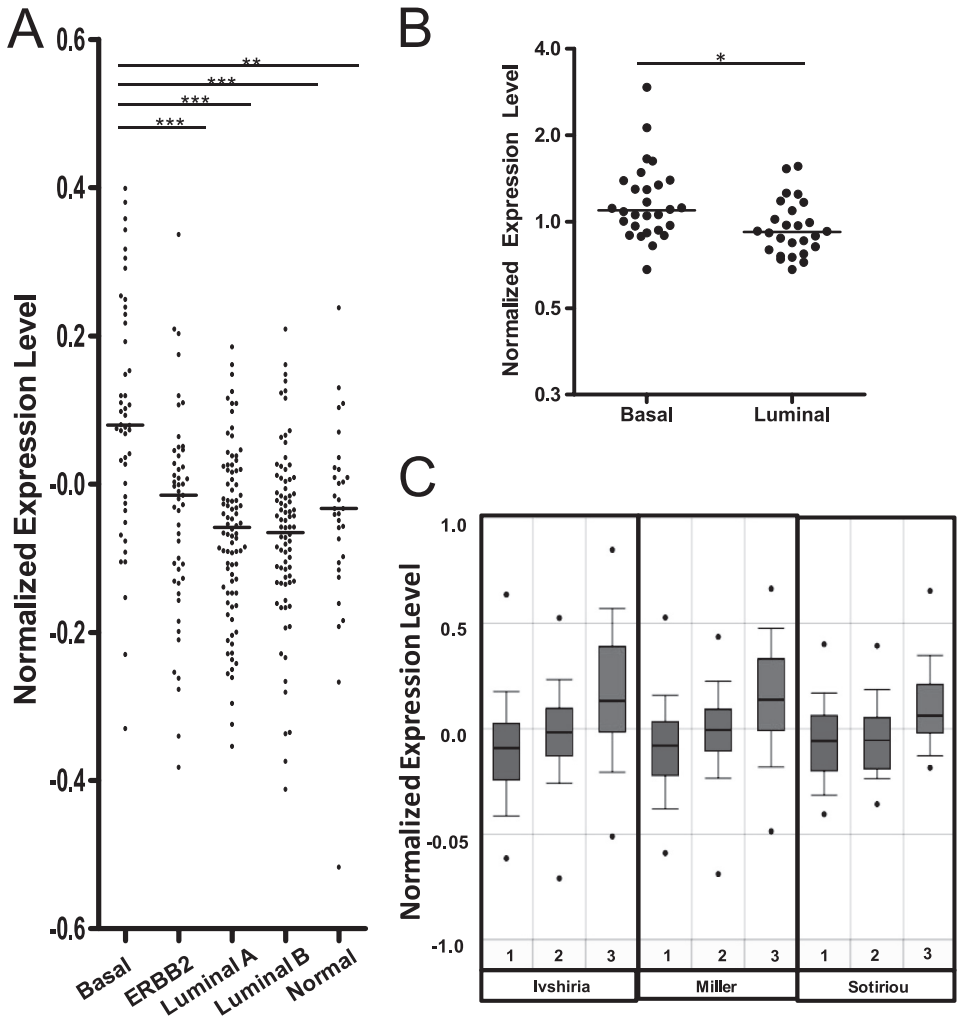

FIGURE 1. **Expression of SPCA1 in breast cancer clinical samples and cell lines.** *A,* relative expression (log_2) of SPCA1 was assessed in a dataset consisting of the microarray profiles of 295 primary breast tumors (33). The gene expression profiles were used to allocate the breast tumors into the five indicated molecular subtypes. *Horizontal lines* represent median values. Significance was measured using a Kruskall-Wallis test with ** indicating $p < 0.01$ and *** indicating $p < 0.001$. *B,* relative SPCA1 expression (log_2) was assessed in a microarray dataset of breast cancer cell lines classified as basal-like ($n = 28$) or luminal ($n = 26$). *Horizontal lines* represent median values. Significance was measured using a Mann-Whitney Test with * indicating $p < 0.01$. *C,* SPCA1 expression was analyzed and visualized using Oncomine™ (Compendia Bioscience, Ann Arbor, MI). In each independent study, an increase in SPCA1 expression was observed in tumors of higher grades as graded by the Elston-Ellis grading method. Ivshiria grade *1 versus 3*, $p < 4.1 \times 10^{-9}$; Miller grade *1 versus 3*, $p < 8.6 \times 10^{-9}$; and Sotiriou grade *1 versus 3*, $p < 1.5 \times 10^{-6}$. *n* values for studies were as follows: grade 1 ($n = 68$), grade 2 ($n = 126$), and grade 3 ($n = 55$); Miller grade 1 ($n = 67$), grade 2 ($n = 128$), and grade 3 ($n = 54$).

(1:10,000; 170–6516; Bio-Rad). For the analysis of the proteolytic processing of IGF1R, the primary antibody was rabbit anti-IGF1R (1:500; sc-713; Santa Cruz Biotechnology) targeted at ER/TGN pro-IGF1R and IGF1Rβ. The secondary antibody was goat anti-rabbit HRP conjugate (1:10,000; 170–6515; Bio-Rad). Bands were visualized with chemiluminescence using Super-Signal West Dura (Thermoscientific). Densitometric data were obtained from pooled data and were acquired using a VersaDoc and Quantity One Analysis software (Bio-Rad). Data were normalized to β-actin and are presented relative to siNT. Line analysis was performed using the Quantity One Analysis software.

Assessment of Viable Cells—MDA-MB-231 cells were assessed for viability after siSPCA1 treatment alone and also in the presence of tunicamycin and siSPCA1. Cells were transfected, and 48-h post-transfection cells were treated with increasing concentrations of tunicamycin for 48 h. Viability was assessed using the CellTiter 96 Aqueous One Cell proliferation assay (Promega) as described previously (36).

Three-dimensional Top of Cell Culture—Microplates (96-well) were coated in Matrigel™ (50 μl; BD Biosciences), and then 6000 cells were plated on top in the absence of antibiotics. Cells were allowed to attach for 6 h prior to treatment with siRNA and then cultured for 96 h with feeding every 2 days. At 24 and 96 h post-transfection, cells were separated from Matrigel™ by incubation in Dispase (62.5 μl; BD Biosciences), then washed, and collected by centrifugation at 300 $\times$ *g* for 5 min prior to RNA isolation. To determine the morphology of cells grown in three-dimensional culture, cells were stained at 96 h with phalloidin Alexa Fluor® 488 (Molecular Probes, Invitrogen), and the nucleus was stained with DAPI (Invitrogen). Images were taken using a Zeiss Axio Imager Z1 microscope with Apotome optical sectioning.

Measurement of Intracellular Calcium—MDA-MB-231 cells were seeded at 4000 cells/well into a 96-well plate and transfected with siRNA. Transfection medium was removed 72 h post-transfection, and cells were loaded with Fluo-4 AM (100 μl; 2 μM; Molecular Probes) in physiological salt solution, 1.8 mM Ca^{2+}, with PBX signal enhancer (PBX calcium assay kit; BD Biosciences) and 500 μM probenecid for 1 h at 37 °C, 5% CO_2. Cells were equilibrated for 15 min to room temperature. Loading solution was removed and replaced with room temperature nominal calcium physiological salt solution (100 μl), PBX signal enhancer solution with 500 μM probenecid, and the plate was placed in the fluorescence imaging plate reader (FLIPR^{TETRA}, Molecular Devices). BAPTA (500 μM; Invitrogen) was added followed by the addition of cyclopiazonic acid (CPA; 10 μM; Sigma). Calcium measurements were taken at 470–495 λ excitation and 515–575 λ emission with the area under the curve from the CPA-induced calcium transient measured from 14.3 to 497.58 s. For the effect of purinergic, PAR1, or PAR2 receptor agonist-mediated cytosolic calcium signaling, ATP (10 μM), thrombin (3.0 units/ml), or trypsin (100 nM), respectively, was added post-BAPTA addition, and the area under the curve was measured from the

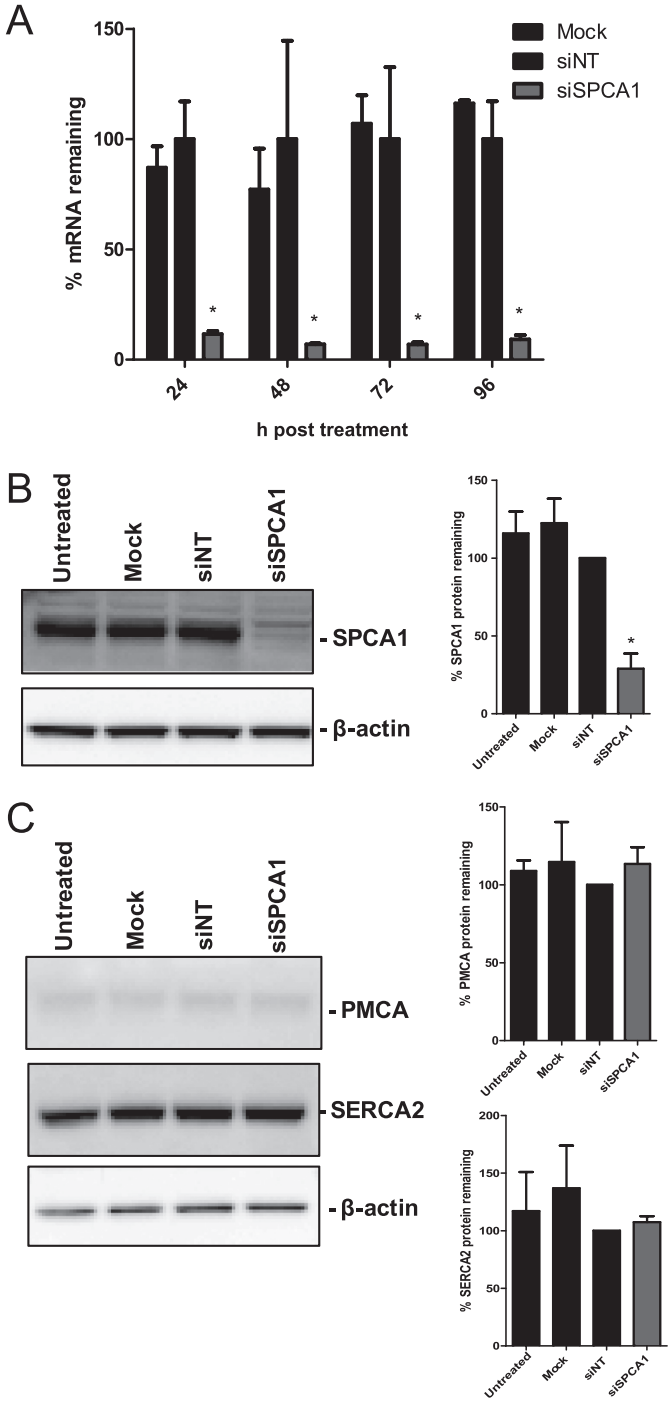

FIGURE 2. **siRNA silencing of SPCA1 in MDA-MB-231 cells.** *A,* quantitation of mRNA for SPCA1 after treatment with SPCA1 siRNA. Statistical analysis was performed using a two-way ANOVA; *, $p < 0.05$ compared with siNT at each time point. *B,* detection of SPCA1 protein post-SPCA1 siRNA treatment. The immunoblot image is a representative blot of three independent experiments. Densitometric data were obtained from the pooled data. Data were normalized to β-actin and are presented relative to siNT as means ± S.E. Statistical analysis was performed using one-way ANOVA; *, $p < 0.05$ compared with siNT. *C,* detection of PMCA and SERCA2 protein post-SPCA1 siRNA treatment.

ATP-, trypsin-, and thrombin-induced calcium transient from 14.3 to 200.15 s.

Statistical Analysis—Unless otherwise stated, data analyses were performed using GraphPad Prism version 4.0 for Windows, and significant differences were analyzed using the appropriate statistical test as described in the figure legends.

RESULTS

We investigated the calcium pump SPCA1 in the context of breast cancer transcriptional subtypes. SPCA1 levels were significantly elevated in clinical samples classified molecularly as belonging to the basal subtype compared with all other subtypes, ERRB2, luminal A, luminal B, and normal (Fig. 1*A*). The association between SPCA1 and the basal subtype was further strengthened by the significant elevation of SPCA1 levels in breast cancer cell lines classified as basal-like compared with those classified as luminal (Fig. 1*B*). SPCA1 levels were also elevated with increasing tumor grade (Fig. 1*C*). Because of this association between SPCA1 levels and the basal subtype, we explored the consequences of SPCA1 inhibition in the basal-like MDA-MB-231 breast cancer cell line.

MDA-MB-231 cells treated with siRNA to SPCA1 had significantly reduced levels of SPCA1 mRNA, which was maintained up to 96 h post-treatment (Fig. 2*A*) and significantly reduced SPCA1 protein at 72 h post-silencing (Fig. 2*B*). MDA-MB-231 cells express only the SPCA1 isoform. To ensure there was no compensatory change in other p-type Ca^{2+}-ATPases, as seen in COS-7 cells stably overexpressing rat SPCA1 (37), we also measured the effects of SPCA1 siRNA on the plasma membrane ATPase (PMCA) and the sarcoplasmic/endoplasmic reticulum Ca^{2+}-ATPase SERCA2, neither of which were significantly altered (Fig. 2*C*).

Inhibition of SPCA1 expression significantly reduced the proliferation of MDA-MB-231 cells 96 h post-siRNA treatment (Fig. 3*A*). We also examined the effect of SPCA1 siRNA on cellular morphology in three-dimensional Matrigel cultures as assessed through phalloidin staining (34). Knockdown of SPCA1 in three-dimensional cultures of MDA-MB-231 cells (Fig. 3*B*) did not reduce cell viability at 96 h (Fig. 3*C*) nor at later time points (data not shown). Knockdown was associated with the acquisition of a more rounded appearance of cells and a reduction in the cell density of colonies (Fig. 3*D*). Altered cellular morphology was accompanied by actin rearrangement (Fig. 3*D, bottom panels*).

To explore one possible mechanism for the consequences of SPCA1 inhibition in MDA-MB-231 cells, the effects of siSPCA1 on tunicamycin-mediated inhibition of MDA-MB-231 viability was assessed. There was a dose-dependent decrease in the relative number of MDA-MB-231 cells after tunicamycin treatment; however, inhibition of SPCA1 expression did not sensitize MDA-MB-231 cells to this agent (Fig. 4*A*). Similarly, levels of the endoplasmic reticulum stress marker GRP94 (39) were increased with tunicamycin treatment, but this was not enhanced by SPCA1 knockdown (Fig. 3*B*). Assessment of endoplasmic reticulum calcium regulation with SPCA1 inhibition was determined via the measurement of $[Ca^{2+}]_{CYT}$ increases mediated by the sarco/ER calcium ATPase inhibitor CPA. We saw a modest decrease in peak calcium and the area under the $[Ca^{2+}]_{CYT}$ transient curve with SPCA1 silencing (Fig. 4, *C* and *D*).

A change in endoplasmic reticulum calcium handling may arise via global alterations in cytosolic calcium homeostasis

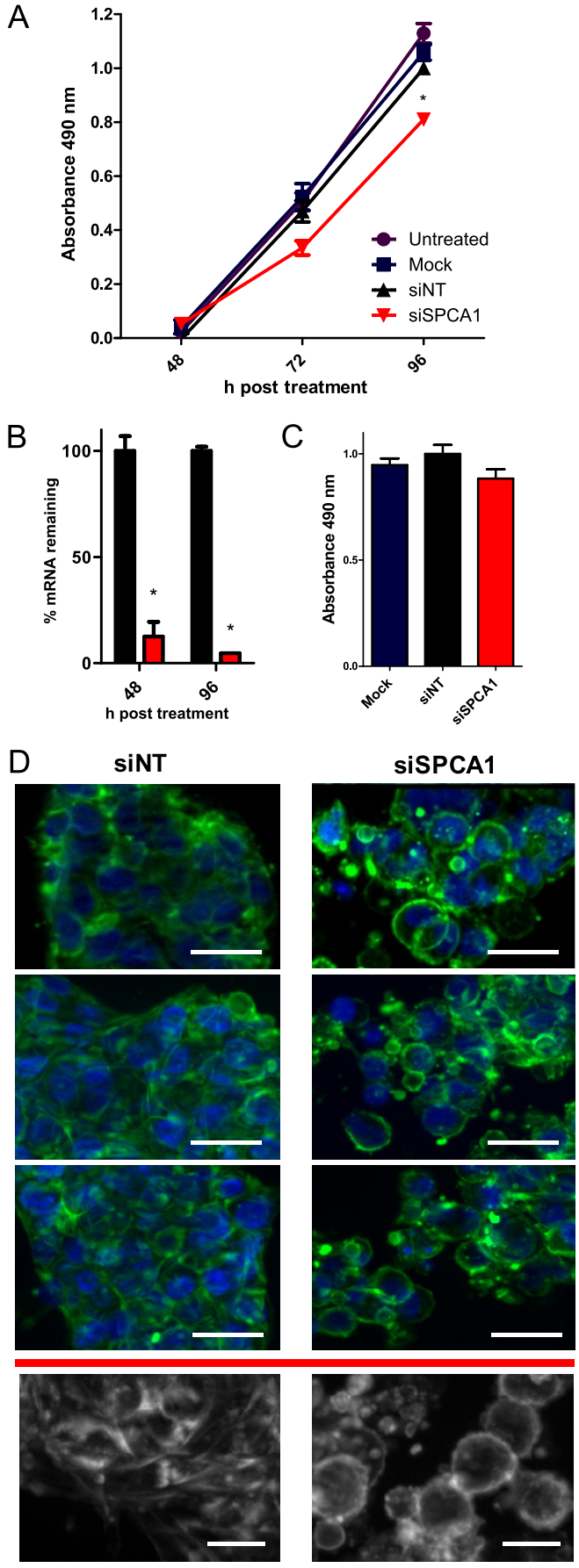

associated with SPCA1 inhibition. To investigate this hypothesis, we examined G-protein-coupled receptor agonist-mediated calcium release from intracellular Ca^{2+} stores. Cells were first stimulated with the purinergic receptor activator ATP in the absence of extracellular calcium. SPCA1 knockdown caused no significant alteration in peak calcium, area under the curve, or the nature of the calcium transient with this stimulus compared with controls (Fig. 5*A*). We also assessed the effects of siSPCA1 in MDA-MB-231 on thrombin and trypsin and PAR1 and PAR2 activators, respectively (38). We resolved a modest but significant effect of SPCA1 knockdown, with reductions in the peak $[Ca^{2+}]_{CYT}$ achieved after stimulation and in the area under the curve (Fig. 5, *B* and *C*).

Although the effects on PAR signaling would be unlikely to explain the phenotypes induced by SPCA1 knockdown in MDA-MB-231 cells, the dependence of PAR1 and PAR2 activity on post-translational modification (38) prompted us to directly evaluate the possible effects of SPCA1 inhibition on the processing of proteins that reside in the secretory pathway and that are important in cancer. Production of functional IGF1R in MDA-MB-231 cells was used to assess the consequences of SPCA1 silencing. Two pro-forms of IGF1R reside, respectively, in the ER (ER pro-IGF1R) and the trans-Golgi network (TGN pro-IGF1R) (39, 40). TGN pro-IGF1R is proteolytically cleaved in the trans-Golgi network to produce IGF1Rα and IGF1Rβ, which assemble to form a functional heteromeric receptor at the plasma membrane (40). As reported for other cell types, MDA-MB-231 cells under control conditions have detectable levels of ER pro-IGF1R, no detectable levels of the TGN pro-IGF1R, and high levels of the proteolytically cleaved functional form IGF1Rβ (Fig. 6*A*) (41, 42). Silencing of SPCA1 resulted in a pronounced decrease (~80%) in the production of IGF1Rβ relative to controls and the pronounced accumulation of TGN pro-IGF1R, which was previously undetectable (Fig. 6).

DISCUSSION

Despite the proposed importance of the secretory pathway in breast epithelial cells for the enrichment of milk with calcium (43, 44), and the importance of proteins post-translationally modified in the Golgi on breast cancer progression (6), no studies have assessed the potential association between SPCA1 and breast cancer. There have also been very few studies assessing the functional consequences of SPCA1 inhibition on protein

FIGURE 3. **Effect of SPCA1 siRNA silencing on cell growth and morphology in two- and three-dimensional culture.** *A,* viable cell number of MDA-MB-231 cells after treatment with SPCA1 siRNA in two-dimensional culture. Data were pooled from three independent experiments and are means ± S.E. with $n = 11$ or 12. Statistical analysis was performed using one-way ANOVA; *, $p < 0.05$ compared with siNT at 96 h. *B,* quantitation of SPCA1 mRNA in the presence of SPCA1 siRNA when MDA-MB-231 cells are grown in three-dimensional culture (on top of cell culture method). Results are means ± S.E. ($n = 3$); *, $p < 0.0001$ compared with siNT using a one-way ANOVA. *C,* viable cell number of MDA-MB-231 cells 96 h post-transfection cultured in three dimensions. Data were pooled from three independent experiments and are means ± S.E. with $n = 9$–12. *D,* morphology of MDA-MB-231 cells grown in three dimensions on top of cell culture. Cells were stained with phalloidin Alexa Fluor® 488 and the nuclear stain DAPI. Images shown are representative of three to four random fields of view from three wells per treatment, repeated in three independent experiments. Images *above the line* display phalloidin and DAPI staining (*scale bar,* 25 μm). Images *below the line* display phalloidin staining only (*scale bar,* 12.5 μm).

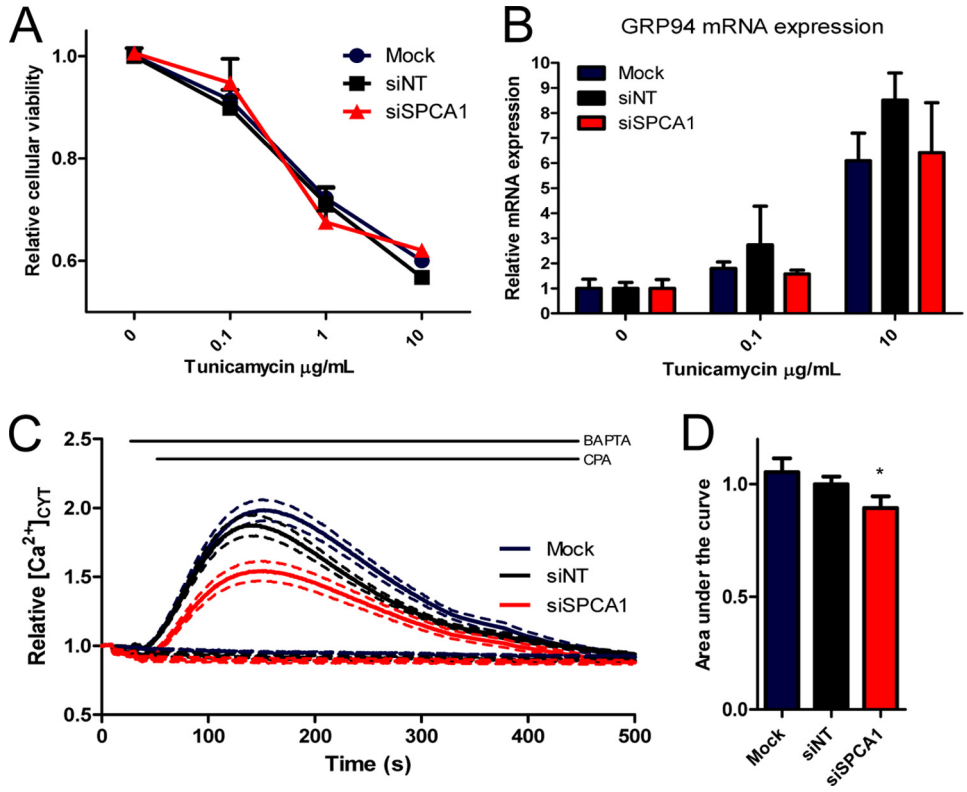

FIGURE 4. *A*, tunicamycin treatment of MDA-MB-231 cells in the presence of SPCA1 siRNA, nontargeting siRNA or transfection agent. Data were normalized to the absence of tunicamycin and are depicted as means ± S.E. ($n = 12$) pooled from three independent experiments. *B*, quantitation of the endoplasmic stress marker GRP94 mRNA using real time RT-PCR. Data were normalized to 18 S rRNA relative to siNT in the absence of tunicamycin and are representative of three independent experiments. Means ± S.E. ($n = 3$). *C*, effect of SPCA1 siRNA on endoplasmic reticulum CPA-mediated calcium transients. Traces display mean fluorescence from 12 individual wells from three independent experiments; *dashed lines* represent means ± S.E. *Bottom traces* represent no CPA controls, and *upper horizontal lines* represent the period of BAPTA or CPA treatment. Individual experiments were normalized to siNT. *D*, area under the curve from the CPA-induced calcium transient from 14.3 to 497.58 s. Data represent means ± S.E. with statistical analysis performed using one-way ANOVA, and * indicates $p < 0.05$ compared with siNT.

post-translational modification in mammalian cells, despite the Ca^{2+} sensitivity of many mammalian Golgi resident enzymes (6). Our studies reported here indicate that SPCA1 overexpression is a characterizing feature of the basal molecular subtype of breast cancer and that changes in its expression can affect the processing of proteins important in tumor progression without major alterations in cytosolic calcium signaling.

SPCA1 knockdown in mice is associated with embryonic lethality (45). Heterozygous animals, however, reach adulthood with no major abnormalities except an increased incidence of squamous cell tumors of the skin and esophagus (45). The absence of a Hailey-Hailey-like disease phenotype in the heterozygous mice (45) implies likely species and cell type-specific consequences of SPCA1 inhibition. Indeed, in COS-1 cells sarco/ER calcium ATPases appear to be the major contributor to calcium accumulation in the Golgi, in contrast to keratinocytes where SPCA1 is the major pathway for Golgi Ca^{2+} sequestration (46). The potential mechanisms for differences between species and predominant effects on skin with SPCA1 and SERCA2 knockdown have been previously discussed (45). The ability of SPCA1 inhibition to reduce tumorigenic pathways in a basal-like human breast cancer cell line while SPCA1 knockdown promotes squamous cell tumors of the skin in mice also reflects species and cell type-specific effects. Despite the phenotype observed in SPCA1 heterozygous animals, SPCA1 does not appear to be a tumor suppressor in humans (45), and in agreement our studies show that in a human breast cancer cell line SPCA1 inhibition is associated with inhibition of breast cancer growth rather than its promotion.

In these studies we assessed potential effects of SPCA1 silencing and the unexplored possible effects on post-translational modification of pro-IGF1R in breast cancer cells. SPCA1 inhibition reduced the proliferation rate of the basal-like breast cancer cell line MDA-MB-231. We also observed alterations in the morphology of these cells in three-dimensional culture (47). Changes in the proliferation and morphology of cells could be indicators of endoplasmic reticulum stress. Silencing of SPCA1 has been associated with increased sensitivity to the secretory pathway stress inducer tunicamycin (24), and SPCA1 null mice exhibit Golgi stress (45); however, SPCA1 silencing in MDA-MB-231 in our studies did not sensitize cells to the effects of tunicamycin and hence is an unlikely mechanism for the observed effects of SPCA1 silencing in this breast cancer cell line.

The effects of SPCA1 inhibition could be mediated by changes in calcium signaling, for example the reduced recovery of $[Ca^{2+}]_{CYT}$ transients leading to the promotion of proliferative pathways. However, the absence of effects of SPCA1 inhibition on ATP-evoked $[Ca^{2+}]_{CYT}$ transients demonstrates a lack of a role for SPCA1 in global $[Ca^{2+}]_{CYT}$ signaling. The localization of SPCA1 to the secretory pathway and thus the potential role in the post-translational modification and trafficking of some proteins could explain differential effects of G-protein-coupled receptor-mediated signaling. However, the only modest effects of SPCA1 inhibition on PAR1 and PAR2 suggest that SPCA1 inhibition does not dramatically alter trafficking or post-translational modifications of these two receptors, and instead other proteins may be more dependent on SPCA1-mediated ion transport for their post-translational modification and activity and be responsible for the observed phenotype seen with SPCA1 knockdown. Our studies have demonstrated that IGF1R is a protein with a key dependence on SPCA1 in MDA-MB-231 breast cancer cells.

IGF1R activity in breast cancer correlates with poor prognosis (7, 28), and the expression of a constitutively active form in

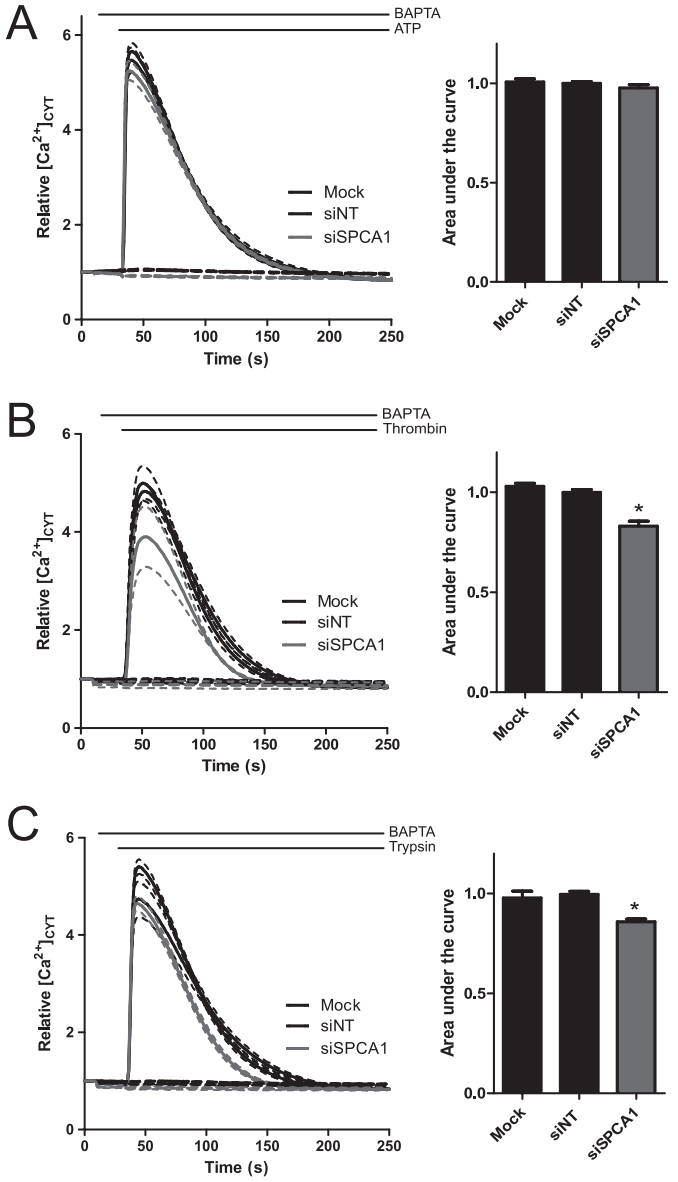

FIGURE 5. **Effect of SPCA1 siRNA on PAR and purinergic receptor agonist-mediated cytosolic calcium signaling and proteolytic processing of IGF1R.** *A,* purinergic receptor agonist ATP-mediated cytosolic calcium signaling. *B,* PAR1 receptor agonist thrombin (3.0 units/ml)-mediated cytosolic calcium signaling; *C,* PAR2 receptor agonist trypsin (100 nM)-mediated cytosolic calcium signaling. For each agonist, traces display mean fluorescence ± S.E. from 11 to 12 individual wells from three independent experiments; *dashed lines* represent S.E., and *bottom traces* represent no agonist controls; *upper horizontal lines* represent the period of BAPTA or agonist treatment. Area under the curve was measured from the ATP-, trypsin-, and thrombin-induced calcium transient from 14.3 to 200.15 s. Individual experiments were normalized to siNT. Statistical analysis was performed using one-way ANOVA, and * indicates $p < 0.05$ compared with siNT.

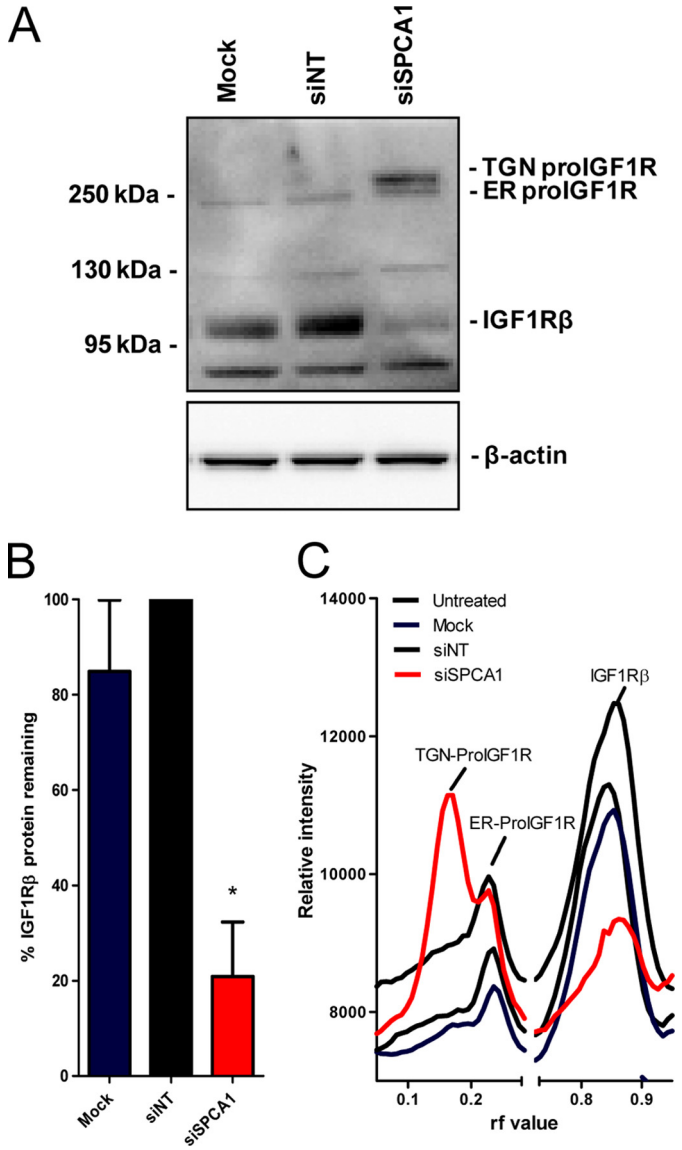

FIGURE 6. **Immunoblot analysis of proteolytic processing of TGN pro-IGF1R.** *A,* representative immunoblot of three independent experiments. *B,* IGF1Rβ density analysis of pooled data with three individual experiments normalized to β-actin and relative to respective siNT control. Statistical analysis was performed using one-way ANOVA; * indicates $p < 0.05$ compared with siNT. *C,* representative line analysis of IGF1R probed immunoblots in the absence of SPCA1 in MDA-MB-231 cells.

mice leads to mammary carcinoma development from 8 weeks after birth (48), whereas inhibiting IGF1R reduces the size of tumors in a mouse model of basal-like breast cancer (30). Clinical trials evaluating the effectiveness of IGF1R inhibitors suggest it is a potential therapeutic target in cancer (49). The molecular pathways involved in IGF1R effects maybe be cancer cell line-dependent but include activation of Akt (48, 50), MAPK phosphorylation (48), and interactions with CXCR4 (51). IGF1R is post-translationally regulated in the trans-Golgi apparatus by the proprotein convertase furin, the activity of which is sensitive to Ca^{2+} (52). Despite the regulation of proprotein convertases by calcium, the possible regulation of these pathways by secretory pathway calcium ATPases has not previously been reported in mammalian cells. Our work highlights SPCA1 as a critical regulator of the generation of IGF1R from its proprotein form in MDA-MB-231 breast cancer cells. IGF1R inhibition, via pharmacological, siRNA, and dominant-negative approaches reduces MDA-MB-231 tumor growth in a NOD/SCID mouse xenograft model (30); hence, IGF1R and its regulation by SPCA1 appears particularly relevant to breast cancers of the basal subtype. Further studies are required to determine whether our observed differences between breast cancer subtypes and within the basal breast cancer cell lines is predictive of their sensitivity to SPCA1 inhibition of IGF1R

processing; such studies should incorporate *in vivo* models of breast cancer cell growth and metastasis.

In summary, breast cancers of the basal subtype are characterized by elevated levels of SPCA1. This is the first time a calcium pump or channel has been associated with the breast cancer molecular subtype associated with the poorest prognosis. Given that regulators of calcium signaling have been identified as potential targets for cancer therapy, calcium transporters associated with basal breast cancers may be particularly significant as there is a shortage of viable therapeutic targets for this breast cancer subtype. Pharmacological inhibitors of SPCA1 may be feasible via chemogenomic approaches based on inhibitors of other similar p-type ATPases (2). Therapeutic approaches designed to alter the regulation of calcium levels within the secretory pathway either through SPCA1 inhibition or other approaches may reduce the activity of calcium-dependent proprotein convertases, previously described as "master switches" in tumor progression (6). The role of these enzymes in the generation of functional IGF1R, TGF-β, and matrix metalloproteinases such as MMP-2 has led proprotein convertases themselves being identified as therapeutic targets for cancer therapy (6). The ability of SPCA1 inhibition to inhibit the generation of functional IGF1R in MDA-MB-231 breast cancer cells, without producing alterations in global calcium signaling, suggests that modifiers of secretory pathway calcium levels may represent unique ways to selectively target proprotein convertase signaling pathways important in tumor progression.

Acknowledgment—We thank Dr. Mina Bissell, Lawrence Berkeley National Laboratory, for the helpful discussions about this work and for hosting H. M. Faddy during her doctoral studies.

REFERENCES

1. Berridge, M. J., Bootman, M. D., and Roderick, H. L. (2003) *Nat. Rev. Mol. Cell Biol.* **4,** 517–529
2. Monteith, G. R., McAndrew, D., Faddy, H. M., and Roberts-Thomson, S. J. (2007) *Nat. Rev. Cancer* **7,** 519–530
3. Roderick, H. L., and Cook, S. J. (2008) *Nat. Rev. Cancer* **8,** 361–375
4. Vangheluwe, P., Sepúlveda, M. R., Missiaen, L., Raeymaekers, L., Wuytack, F., and Vanoevelen, J. (2009) *Chem. Rev.* **109,** 4733–4759
5. Sepúlveda, M. R., Vanoevelen, J., Raeymaekers, L., Mata, A. M., and Wuytack, F. (2009) *J. Neurosci.* **29,** 12174–12182
6. Bassi, D. E., Fu, J., Lopez de Cicco, R., and Klein-Szanto, A. J. (2005) *Mol. Carcinog.* **44,** 151–161
7. Werner, H., and Bruchim, I. (2009) *Arch. Physiol. Biochem.* **115,** 58–71
8. Behne, M. J., Tu, C. L., Aronchik, I., Epstein, E., Bench, G., Bikle, D. D., Pozzan, T., and Mauro, T. M. (2003) *J. Invest. Dermatol.* **121,** 688–694
9. Van Baelen, K., Vanoevelen, J., Missiaen, L., Raeymaekers, L., and Wuytack, F. (2001) *J. Biol. Chem.* **276,** 10683–10691
10. Lissandron, V., Podini, P., Pizzo, P., and Pozzan, T. (2010) *pro-c. Natl. Acad. Sci. U.S.A.* **107,** 9198–9203
11. Ton, V. K., Mandal, D., Vahadji, C., and Rao, R. (2002) *J. Biol. Chem.* **277,** 6422–6427
12. Missiaen, L., Raeymaekers, L., Dode, L., Vanoevelen, J., Van Baelen, K., Parys, J. B., Callewaert, G., De Smedt, H., Segaert, S., and Wuytack, F. (2004) *Biochem. Biophys. Res. Commun.* **322,** 1204–1213
13. Szigeti, R., and Kellermayer, R. (2006) *J. Invest. Dermatol.* **126,** 2370–2376
14. Brini, M., and Carafoli, E. (2009) *Physiol. Rev.* **89,** 1341–1378
15. Porgpermdee, S., Yu, X., Takagi, A., Mayuzumi, N., Ogawa, H., and Ikeda, S. (2005) *J. Dermatol. Sci.* **40,** 137–140
16. Faddy, H. M., Smart, C. E., Xu, R., Lee, G. Y., Kenny, P. A., Feng, M., Rao, R., Brown, M. A., Bissell, M. J., Roberts-Thomson, S. J., and Monteith, G. R. (2008) *Biochem. Biophys. Res. Commun.* **369,** 977–981
17. McManaman, J. L., and Neville, M. C. (2003) *Adv. Drug Deliv. Rev.* **55,** 629–641
18. Reinhardt, T. A., and Lippolis, J. D. (2009) *Biochem. Biophys. Res. Commun.* **378,** 99–102
19. Shennan, D. B. (2008) *Cell. Mol. Biol. Lett.* **13,** 514–525
20. Van Baelen, K., Vanoevelen, J., Callewaert, G., Parys, J. B., De Smedt, H., Raeymaekers, L., Rizzuto, R., Missiaen, L., and Wuytack, F. (2003) *Biochem. Biophys. Res. Commun.* **306,** 430–436
21. Harper, C., Wootton, L., Michelangeli, F., Lefièvre, L., Barratt, C., and Publicover, S. (2005) *J. Cell Sci.* **118,** 1673–1685
22. Nilsson, T., Au, C. E., and Bergeron, J. J. (2009) *FEBS Lett.* **583,** 3764–3769
23. Bates, S., MacCallum, D. M., Bertram, G., Munro, C. A., Hughes, H. B., Buurman, E. T., Brown, A. J., Odds, F. C., and Gow, N. A. (2005) *J. Biol. Chem.* **280,** 23408–23415
24. Ramos-Castañeda, J., Park, Y. N., Liu, M., Hauser, K., Rudolph, H., Shull, G. E., Jonkman, M. F., Mori, K., Ikeda, S., Ogawa, H., and Arvan, P. (2005) *J. Biol. Chem.* **280,** 9467–9473
25. Sohn, Y. S., Park, C. S., Lee, S. B., and Ryu, D. D. (1998) *J. Bacteriol.* **180,** 6736–6742
26. Jones, R. A., and Moorehead, R. A. (2008) *J. Mammary Gland Biol. Neoplasia* **13,** 407–413
27. Yee, D., and Wood, T. L. (2008) *J Mammary Gland Biol. Neoplasia* **13,** 351–352
28. Frasca, F., Pandini, G., Sciacca, L., Pezzino, V., Squatrito, S., Belfiore, A., and Vigneri, R. (2008) *Arch. Physiol. Biochem.* **114,** 23–37
29. Maor, S., Yosepovich, A., Papa, M. Z., Yarden, R. I., Mayer, D., Friedman, E., and Werner, H. (2007) *Cancer Lett.* **257,** 236–243
30. Klinakis, A., Szabolcs, M., Chen, G., Xuan, S., Hibshoosh, H., and Efstratiadis, A. (2009) *pro-c. Natl. Acad. Sci. U.S.A.* **106,** 2359–2364
31. Sørlie, T., Perou, C. M., Tibshirani, R., Aas, T., Geisler, S., Johnsen, H., Hastie, T., Eisen, M. B., van de Rijn, M., Jeffrey, S. S., Thorsen, T., Quist, H., Matese, J. C., Brown, P. O., Botstein, D., Eystein Lønning, P., and Børresen-Dale, A. L. (2001) *pro-c. Natl. Acad. Sci. U.S.A.* **98,** 10869–10874
32. Haupt, B., Ro, J. Y., and Schwartz, M. R. (2010) *Arch. Pathol. Lab. Med.* **134,** 130–133
33. van de Vijver, M. J., He, Y. D., van't Veer, L. J., Dai, H., Hart, A. A., Voskuil, D. W., Schreiber, G. J., Peterse, J. L., Roberts, C., Marton, M. J., Parrish, M., Atsma, D., Witteveen, A., Glas, A., Delahaye, L., van der Velde, T., Bartelink, H., Rodenhuis, S., Rutgers, E. T., Friend, S. H., and Bernards, R. (2002) *N. Engl. J. Med.* **347,** 1999–2009
34. Kenny, P. A., Lee, G. Y., Myers, C. A., Neve, R. M., Semeiks, J. R., Spellman, P. T., Lorenz, K., Lee, E. H., Barcellos-Hoff, M. H., Petersen, O. W., Gray, J. W., and Bissell, M. J. (2007) *Mol. Oncol.* **1,** 84–96
35. Neve, R. M., Chin, K., Fridlyand, J., Yeh, J., Baehner, F. L., Fevr, T., Clark, L., Bayani, N., Coppe, J. P., Tong, F., Speed, T., Spellman, P. T., DeVries, S., Lapuk, A., Wang, N. J., Kuo, W. L., Stilwell, J. L., Pinkel, D., Albertson, D. G., Waldman, F. M., McCormick, F., Dickson, R. B., Johnson, M. D., Lippman, M., Ethier, S., Gazdar, A., and Gray, J. W. (2006) *Cancer Cell* **10,** 515–527
36. Aung, C. S., Ye, W., Plowman, G., Peters, A. A., Monteith, G. R., and Roberts-Thomson, S. J. (2009) *Carcinogenesis* **30,** 1962–1969
37. Reinhardt, T. A., Horst, R. L., and Waters, W. R. (2004) *Am. J. Physiol. Cell Physiol.* **286,** C164–C169
38. Kamath, L., Meydani, A., Foss, F., and Kuliopulos, A. (2001) *Cancer Res.* **61,** 5933–5940
39. Ullrich, A., Gray, A., Tam, A. W., Yang-Feng, T., Tsubokawa, M., Collins, C., Henzel, W., Le Bon, T., Kathuria, S., Chen, E., *et al.* (1986) *EMBO J.* **5,** 2503–2512
40. Khatib, A. M., Siegfried, G., Chrétien, M., Metrakos, P., and Seidah, N. G. (2002) *Am. J. Pathol.* **160,** 1921–1935
41. Khatib, A. M., Siegfried, G., Prat, A., Luis, J., Chrétien, M., Metrakos, P., and Seidah, N. G. (2001) *J. Biol. Chem.* **276,** 30686–30693
42. Lehmann, M., André, F., Bellan, C., Remacle-Bonnet, M., Garrouste, F., Parat, F., Lissitsky, J. C., Marvaldi, J., and Pommier, G. (1998) *Endocrinology* **139,** 3763–3771
43. Lee, W. J., Monteith, G. R., and Roberts-Thomson, S. J. (2006) *Biochim.*

Biophys. Acta **1765,** 235–255
44. Reinhardt, T. A., and Horst, R. L. (1999) *Am. J. Physiol.* **276,** C796–C802
45. Okunade, G. W., Miller, M. L., Azhar, M., Andringa, A., Sanford, L. P., Doetschman, T., Prasad, V., and Shull, G. E. (2007) *J. Biol. Chem.* **282,** 26517–26527
46. Callewaert, G., Parys, J. B., De Smedt, H., Raeymaekers, L., Wuytack, F., Vanoevelen, J., Van Baelen, K., Simoni, A., Rizzuto, R., and Missiaen, L. (2003) *Cell Calcium* **34,** 157–162
47. Fairclough, R. J., Lonie, L., Van Baelen, K., Haftek, M., Munro, C. S., Burge, S. M., and Hovnanian, A. (2004) *J. Invest. Dermatol.* **123,** 67–71
48. Carboni, J. M., Lee, A. V., Hadsell, D. L., Rowley, B. R., Lee, F. Y., Bol, D. K., Camuso, A. E., Gottardis, M., Greer, A. F., Ho, C. P., Hurlburt, W., Li, A., Saulnier, M., Velaparthi, U., Wang, C., Wen, M. L., Westhouse, R. A., Wittman, M., Zimmermann, K., Rupnow, B. A., and Wong, T. W. (2005) *Cancer Res.* **65,** 3781–3787
49. Rodon, J., DeSantos, V., Ferry, R. J., Jr., and Kurzrock, R. (2008) *Mol. Cancer Ther.* **7,** 2575–2588
50. Sachdev, D., Zhang, X., Matise, I., Gaillard-Kelly, M., and Yee, D. (2010) *Oncogene* **29,** 251–262
51. Akekawatchai, C., Holland, J. D., Kochetkova, M., Wallace, J. C., and McColl, S. R. (2005) *J. Biol. Chem.* **280,** 39701–39708
52. Thomas, G. (2002) *Nat. Rev. Mol. Cell Biol.* **3,** 753–766